

RESEARCH ARTICLE

Metal-Supported Mesoporous Aluminosilicate Catalysts for Selective Catalytic Decomposition

Zahra Amirsardari^{*1}, Babak Afzali¹, Mohammad Reza Amirsoleimani¹

¹ Space Transportation Research Institute, Iranian Space Research Center, Tehran, Iran

ABSTRACT

ARTICLE INFO

Article History:

Received 2023-10-15

Accepted 2024-11-23

Published 2023-09-15

Keywords:

Catalyst,

Aluminosilicate,

Support,

Iridium nanoparticles,

Decomposition parameters.

Iridium catalysts with the active component content of 10, 20, and 30 wt% on mesoporous aluminosilicate have been synthesized by the reductive hydrolysis of iridium chloro complexes. The degree of dispersion of supported iridium was controlled by increasing the weight percentage of iridium nanoparticles in the catalyst. In this research, it was shown that the crushing strength of the catalysts synthesized on the basis of aluminosilicate with different weight percentages of iridium nanoparticles can be different. The results of hydrazine decomposition show that the performance of the catalysts increases from 10 wt% to 20 wt%, and subsequently, by increasing the concentration of iridium to 30% by weight, with the decomposition parameters remaining constant, the resistance to crushing of the catalyst decreases. The present work is intended to provide some useful correlations between the iridium catalytic activity and the potential parameters in the support materials, and thus making the process more active.

How to cite this article

Amirsardari Z., Afzali B., Amirsoleimani M. R., *Metal-Supported Mesoporous Aluminosilicate Catalysts for Selective Catalytic Decomposition*. *J. Nanoanalysis.*, 2023; 10(3): 584-591.

INTRODUCTION

*Corresponding Author Email: Z.Amirsardari@isrc.ac.ir



This work is licensed under the Creative Commons Attribution 4.0 International License.

To view a copy of this license, visit <http://creativecommons.org/licenses/by/4.0/>.

Significant challenges remain to increase the activity and stability of catalysts for hydrazine degradation (1,2). In addition, new innovative technical solutions should be applied in the decomposition process to overcome the economic concerns about catalyst deactivation and degradation (3,4). This means that a suitable, reliable, stable and economical catalyst should be developed to cover the gap between laboratory and industrial implementation (5). Catalyst supports play a dominant role in enhancing the properties of the active metal phase in catalytic decomposition processes (6–8).

Decomposition of hydrazine is performed on a heterogeneous catalyst, which theoretically starts at the interface between the catalyst surface and N_2H_4 molecules (9). Therefore, the performance of a hydrazine decomposition catalyst should be related to the nature, concentration and accessibility of active sites on the catalyst surface (10). These parameters are probably affected by the factors including preparation conditions of the iridium catalyst, the operating parameters of synthesis, support surface, and structural properties (11,12). All of these factors can play a major role in the structure of surface species. Gamma alumina is the most important and cheapest support (13,14). Unlike alumina, the silica support surface contains hydroxyl groups, which do not exhibit Brønsted acidity, but its acidity is regulated by the incorporation of Al into the silica, so that weak to moderately acidic sites can be created (15,16). The molecular nature of the interaction of the surface functions of silica and alumina with metal centers affects the performance of the catalyst.

Although different alumina-silica supports have been used for different catalysts, unlike alumina supports, the weight percentages of iridium for different applications have not been studied on. Iridium active 20 to 40% by weight has been used as

a catalyst on alumina supports for hydrazine decomposition (17–20). But the effects of iridium on other inexpensive supports, such as aluminosilicate, have not been used in the decomposition of hydrazine. The resistance to mechanical and thermal stresses can be optimized by controlling the loading of nanoparticles inside the pores of the catalyst support, and the rate of hydrazine decomposition can be changed to the desired level. Therefore, the amount of catalyst loading on a specific support is very important in its performance characteristics (21–23).

To date, no studies have been conducted on the hydrazine decomposition process at industrially used weight percentages including 10–30 wt% of iridium catalysts on aluminosilicate support at atmospheric pressure. The rate of movement of hydrazine strongly depends on the surface conditions of the catalyst. Effect of support is discussed in the present work, with particular focus on the catalytic activity for hydrazine decomposition. The present work is intended to provide some useful correlations between the iridium catalytic activity and the potential parameters in the support materials, and thus making the process more active. A clear difference in catalytic performance in terms of activity and hydrogen selectivity was seen for catalysts with silica and alumina supports for the hydrazine reaction.

EXPERIMENTAL

Preparation of catalysts

Dihydrogen hexachloroiridate (IV) hydrate ($H_2IrCl_6 \cdot xH_2O$, Sigma-Aldrich) was dissolved in the deionized water for 24 h. Subsequently, quantitative aluminosilicate supports (grain diameter 1-2 mm), were introduced into the above mixed solution under stirring and shaking. The supports were impregnated into the iridium aqueous solution, after being fully

impregnated; a solvent evaporation process was conducted at 60°C. Each impregnation step was carried out with 5% by weight of iridium for each step of the synthesis catalyst. The resulting granules were dried at 60°C, and then the oven temperature was set at 80°C for 24h to conduct solvent evaporation. Finally, the granules underwent a calcination process: the temperature was increased from 30 to 400°C (1°C. min⁻¹ ramp rate) and held for 3h, and then H₂-reduction of catalysts at 400°C done with the formation of iridium active phases. The obtained samples were denoted as AlSi, 10Ir@AlSi, 20Ir@AlSi, and 30Ir@AlSi for corresponding iridium content (0, 10, 20, and 30 by weight of iridium on the support of aluminosilicate). Three types of catalysts were used for the decomposition of hydrazine monohydrate in a laboratory reactor.

Characterization of catalysts

The N₂ adsorption-desorption experiments were conducted to investigate the textural properties of samples through BELSORP-Mini, MicrotracBel Corp. analyser by preconditioning at 150°C in inert gas for 5h. The analysis of reduced catalysts was performed. A FE-SEM microscope Model, Zeiss-

RESULTS AND DISCUSSION

Fig. 1 and Table 1 show the adsorption-desorption isotherms of the iridium-aluminosilicate catalysts. The surface area of the aluminosilicate support is about 14 cm²/g. The specific surface area of aluminosilicate coated with iridium determined by BET and mean size of the micro pores decreased with an increase in the thickness of the deposited iridium layer due to the blockage of some pores with iridium nanoparticles. The specific surface area per gram of the deposited iridium (30 wt %) was almost

Fig. 2 shows a typical image of iridium on the aluminosilicate catalyst surface, obtained by SEM. The growth and dispersion of iridium particles occur during the process at all available surfaces. As

SIGMA VP, Germany was used. The catalytic performance on hydrazine monohydrate decomposition was evaluated by placing 0.1 g catalyst into a sealed stainless steel laboratory reactor equipped with the temperature (T) and pressure (P) sensors under atmospheric pressure at 25°C. The mixed reaction gas included NH₃, N₂, and H₂ passed through a trap containing 1 M HCl to absorb ammonia. The reaction product was collected through a cylinder by the water displacement method and recorded by a computer program. The moles number and hydrogen selectivity (X) can be calculated by equation (1):

$$X = \frac{3\lambda - 1}{8} \left[\lambda = \frac{n(\text{N}_2) + n(\text{H}_2)}{n(\text{N}_2\text{H}_4)} \right] \quad (1)$$

TOF or the reaction rate (h⁻¹) in 80% conversion of hydrazine hydrate was obtained as follows:

$$\text{TOF} = \frac{PV}{3n_{\text{metal}}RTt} \quad (2)$$

where, R is the universal gas constant, T is the reaction temperature, P is the atmospheric pressure, n_{metal} is the mole number of iridium, V is the volume of H₂ and N₂, and t is the reaction time.

two times higher than that of the aluminosilicate support. Low level of accumulation resulting from increasing iridium loading increased the BET surface area of 30Ir@AlSi catalyst through the well-controlled deposition of iridium onto the aluminosilicate support. Since the surface areas of the 10 and 20 wt% catalyst samples in this study ranged between 12 and 15 m². g⁻¹, there was no significant change in surface areas. The increase of the active phase causes the blockage of support pores from 14 nm to 5 nm with iridium nanoparticles during impregnation.

it could be seen in Fig. 2 a and b, the irregular iridium nanoparticles with wide distribution of pore sizes is observed. These images clearly show that the particles adhered together. The particles with an

average size of about 50– 100 nm are predominant. Iridium particles on 30Ir@AlSi catalyst have low size distribution (<50nm), and they have relatively uniform distribution on the support surface. The deposition of iridium particles takes place not only

on support surface, but also in the pores. The deposited iridium particles were found to be well dispersed with the control on the number of impregnation steps.

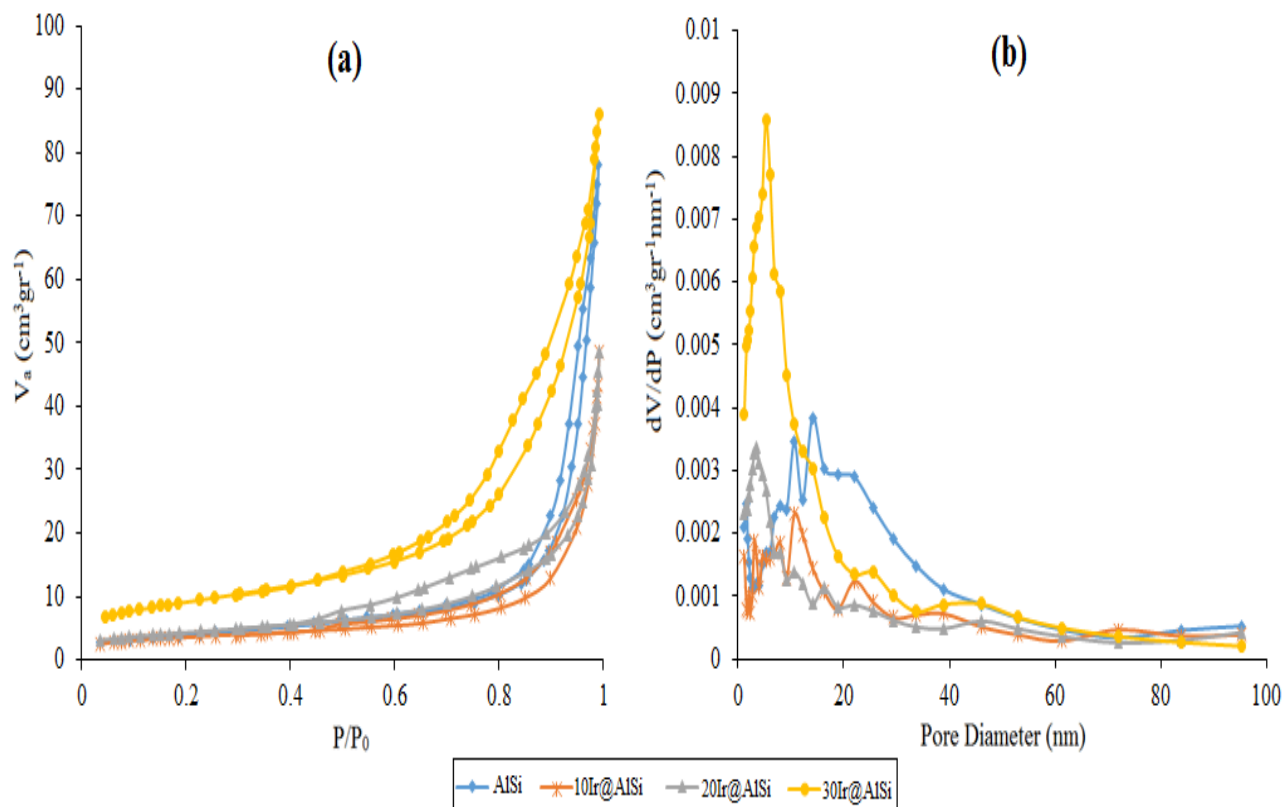


Fig. 1. (a) Nitrogen adsorption–desorption isotherms and (b) pore size distribution curves for the iridium@aluminosilicate catalysts

Table 1. BET properties of catalysts with different iridium contents on aluminosilicate supports

Composition	S_{BET} (m^2g^{-1})	Pore volume (cm^3/g)	Pore Diameter (nm)
AlSi	14	0.12	14
10Ir@AlSi	12	0.06	10
20Ir@AlSi	15	0.06	3
30Ir@AlSi	32	0.13	5

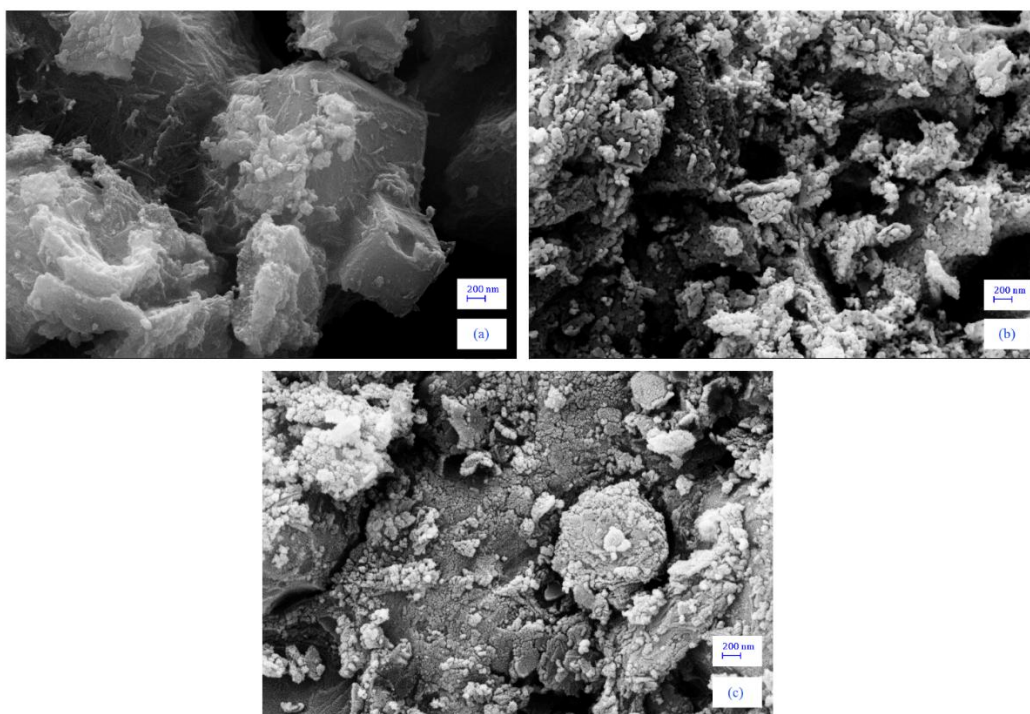


Fig. 2. FE-SEM images of the catalysts with (a) 10 wt%, (b) 20 wt%, and (c) 30 wt% of iridium nanoparticles on aluminosilicate supports.

The comparison of the efficiency of the catalyst decomposition test of 10, 20 and 30% by weight of iridium on the support of aluminosilicate shows that with the increase of the amount of metal from 10 to 20% by weight, the amount of moles of the resulting gases has increased (Fig. 3a.). However, the rate of ammonia decomposition, hydrogen selectivity and catalyst reaction rate remained constant from 20 to 30 wt% according to Fig. 3b. It has been expected that with the increase in the amount of metal from 20 to 30 wt%, a large increase will be observed (due to the increase in the amount of iridium). But this amount was not seen and almost the ratios obtained from the analysis were the same for 20 and 30% by weight of iridium, with the difference that in 30% by weight, about 49% of crushing was seen after the test. Cracks were formed on the 30% catalyst granules during the calcination process due to the high volume of water vapour escaping from the holes. The distribution of nanoparticles on supports containing

aluminosilicate is less orderly than that of alumina (24), and the distribution is not uniform, the accumulation of particles in the holes causes a large volume of water vapour to escape during calcination. Finally, water vapour pressure causes cracks. With the production of gases at a high speed resulting from the decomposition of hydrazine monohydrate during the process, the resulting cracks cause 49% crushing. The decomposition test was performed very slowly with 10% by weight of iridium nanoparticles on the aluminosilicate support, and the test continued even after one hour and progressed very slowly with a speed of approximately 3.5 times less than 20% by weight of iridium. Therefore, the percentage of ammonia decomposition and selectivity to hydrogen could not be calculated. Due to this low reaction speed and slow release of gases, the crushing in this weight percentage reached 20%. In 20% by weight of iridium, no crushing was seen and the speed and percentage of ammonia decomposition and

selectivity to hydrogen were better than other percentages. After the catalysts were used for hydrazine decomposition, the SEM images of the sample were investigated in Fig. 4. From the SEM inspections of the catalysts before and after reaction, we can see that the phase of the samples did not

change and the morphology has remained to some extent. Little changes in the morphology of catalyst surfaces may be because of the effect of external force, such as product gases for decomposition of hydrazine monohydrate. So, the as-prepared iridium catalysts are stable as a solid phase catalyst.

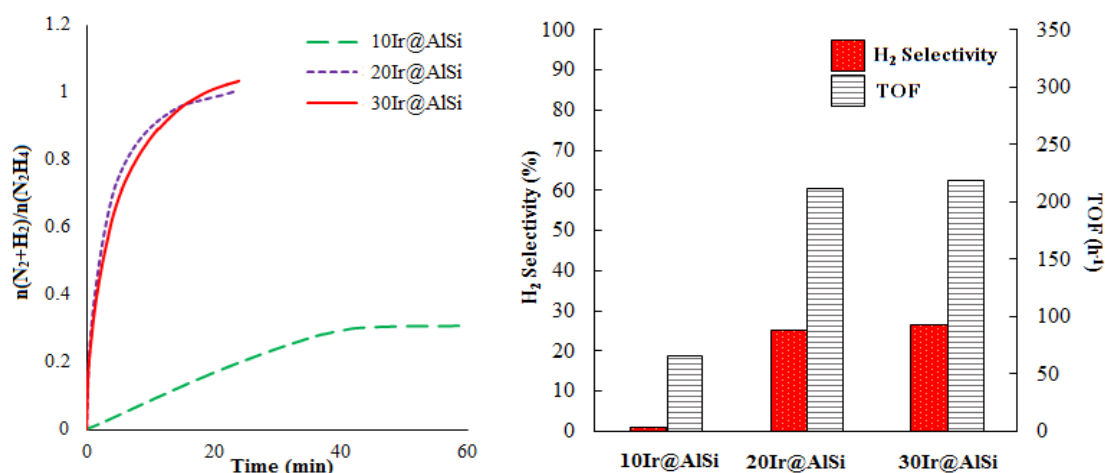


Fig. 3. (a) Time profiles and (b) selectivity and TOF values for decomposition of hydrazine monohydrate catalyzed by the iridium@aluminosilicate

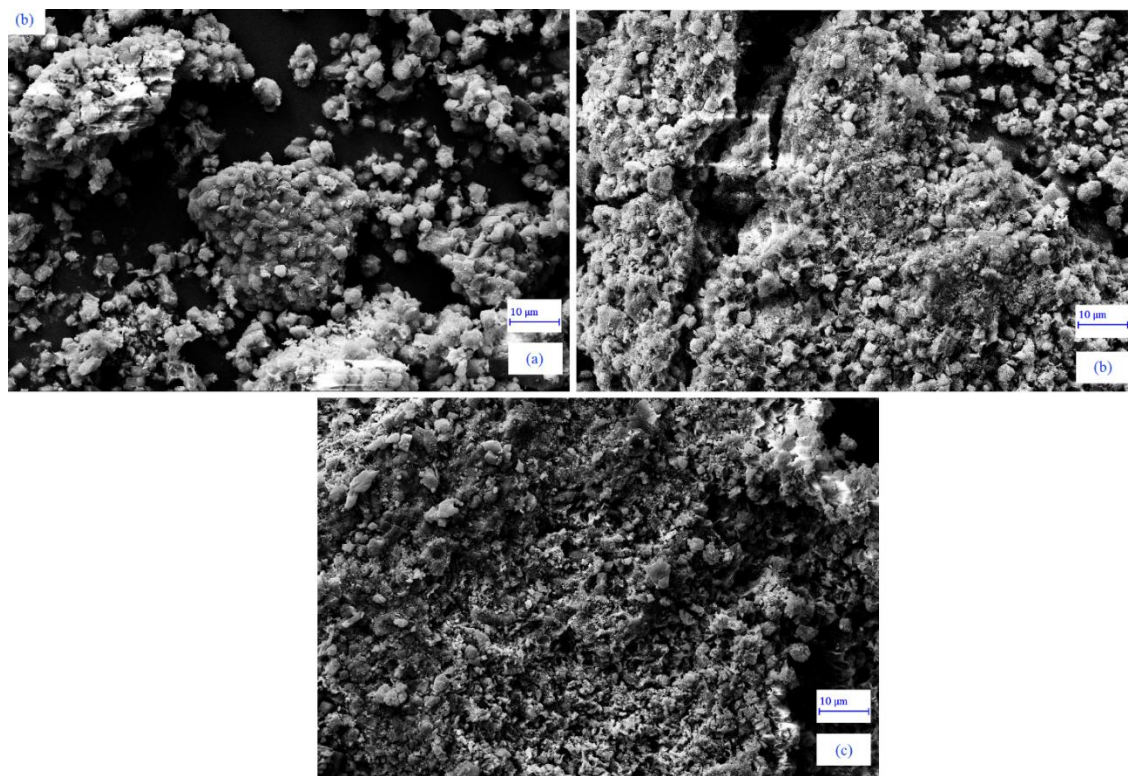


Fig. 4. FE-SEM images of the catalysts with (a) 10 wt%, (b) 20 wt%, and (c) 30 wt% of iridium nanoparticles on aluminosilicate supports after decomposition of hydrazine monohydrate

CONCLUSION

Optimizing the loading level of active phase on aluminosilicate supported with proper catalytic activity is needed in hydrazine decomposition. Catalysts with 20% and 30% by weight on aluminosilicate granules showed higher hydrazine decomposition rates and resulted in more hydrogen and nitrogen gas products, thus providing the most efficient decomposition process. However, a significant difference was observed in the analysis process between 10% by weight and the other two percent of the samples. Also, in the catalyst with 30% by weight of nanoparticles, with the production of gases resulting from the decomposition of hydrazine at a high speed during the process, the resulting cracks cause 49% of it to be crushed. Therefore, the 20% by weight catalyst with high activity and stronger mechanical strength is a more suitable option for hydrazine decomposition.

REFERENCES

- [1]. Tang P, Wen H, Wang P. Hierarchically nanostructured $\text{Ni}_2\text{Fe}_2\text{N}$ as an efficient electrocatalyst for hydrazine oxidation reaction. *Chem Eng J*. 2022;431:134123.
- [2]. P. Yang, L. Yang, Q. Gao, Q. Luo, X. Zhao, X. Mai, Q. Fu, M. Dong, J. Wang YH. Anchoring carbon nanotubes and post-hydroxylation treatment enhanced Ni nanofiber catalysts towards efficient hydrous hydrazine decomposition for effective hydrogen generation. *Chem Commun*. 2019;55(61):9011–4.
- [3]. Amirsardari Z, Dourani A, Amirifar MA, Ghadiri Massoom N, Afzali B. Distribution and grain size support-dependent catalytic properties of iridium nanoparticles. *J Nanoanalysis*. 2021;8(3):199–208.
- [4]. Zhang M, Liu L, Lu S, Xu L, An Y, Wan C. Facile fabrication of NiPt/CNTs as an efficient catalyst for hydrogen production from hydrous hydrazine. *ChemistrySelect*. 2019;4(35):10494–500.
- [5]. Amirsardari Z, Dourani A, Amirifar MA, Massoom NG. Comparative characterization of iridium loading on catalyst assessment under different conditions. *Int J Miner Metall Mater*. 2021;28(7):1233–9.
- [6]. Zhang W, Xia S, Chen C, He H, Jin Z, Luo M, et al. Understanding the crucial roles of catalyst properties in ethyl acetate and toluene oxidation over Pt catalysts. *New J Chem*. 2021;45(25):11352–8.
- [7]. Long D, Chen Q, Qiao W, Zhan L, Liang X, Ling L. Three-dimensional mesoporous carbon aerogels: ideal catalyst supports for enhanced H_2S oxidation. *Chem Commun*. 2009;(26):3898–900.
- [8]. Salavati-Niasari M, Bazarganipour M. Synthesis, characterization and catalytic oxidation properties of multi-wall carbon nanotubes with a covalently attached copper (II) salen complex. *Appl Surf Sci*. 2009;255(17):7610–7.
- [9]. Lu X, Francis S, Motta D, Dimitratos N, Roldan A. Mechanistic study of hydrazine decomposition on Ir (111). *Phys Chem Chem Phys*. 2020;
- [10]. Amirsardari Z, Dourani A, Hasanpour F, Amirifar MA, Ghadiri N. Effect of silica content on support-iridium active phase interactions on the nanocatalyst activity. *J Nanostructures*. 2020;10(2):348–61.
- [11]. Bellomi S, Barlocco I, Chen X, Delgado JJ, Arrigo R, Dimitratos N, et al. Enhanced stability of sub-nanometric iridium decorated graphitic carbon nitride for H_2 production upon hydrous hydrazine decomposition. *Phys Chem Chem Phys*. 2023;25(2):1081–95.
- [12]. Matyshak VA, Silchenkova ON. Catalytic

decomposition of hydrazine and hydrazine derivatives to produce hydrogen-containing gas mixtures: a review. *Kinet Catal.* 2022;63(4):339–50.

[13]. Sanchez SI, Menard LD, Bram A, Kang JH, Small MW, Nuzzo RG, et al. The emergence of nonbulk properties in supported metal clusters: negative thermal expansion and atomic disorder in Pt nanoclusters supported on γ -Al₂O₃. *J Am Chem Soc.* 2009;131(20):7040–54.

[14]. Namvar F, Hajizadeh-Oghaz M, Mahdi MA, Ganduh SH, Meshkani F, Salavati-Niasari M. The synthesis and characterization of Ni-M-Tb/Al₂O₃ (M: Mg, Ca, Sr and Ba) nanocatalysts prepared by different types of doping using the ultrasonic-assisted method to enhance CO₂ methanation. *Int J Hydrogen Energy.* 2023;48(10):3862–77.

[15]. Joshi P, Huang H-H, Yadav R, Hara M, Yoshimura M. Boron-doped graphene as electrocatalytic support for iridium oxide for oxygen evolution reaction. *Catal Sci Technol.* 2020;10(19):6599–610.

[16]. Hauser JL, Amberchan G, Tso M, Manley R, Bustillo K, Cooper J, et al. A mesoporous aluminosilicate nanoparticle-supported nickel–boron composite for the catalytic reduction of nitroarenes. *ACS Appl Nano Mater.* 2019;2(3):1472–83.

[17]. Li L, Wang X, Zhao X, Zheng M, Cheng R, Zhou L, et al. Microcalorimetric studies of the iridium catalyst for hydrazine decomposition reaction. *Thermochim Acta.* 2005;434(1–2):119–24.

[18]. Salimi M, Pakdehi SG, Shekarian A. Ir impregnation on alumina pores: catalyst activity and loss during hydrazine decomposition. *Propellants, Explos Pyrotech.* 2020;

[19]. Pakdehi SG, Rasoolzadeh M. Comparison of catalytic behavior of iridium and nickel nanocatalysts for decomposition of hydrazine. *Procedia Mater Sci.* 2015;11:749–53.

[20]. Jang IJ, Shin HS, Shin NR, Kim SH, Kim SK, Yu MJ, et al. Macroporous–mesoporous alumina supported iridium catalyst for hydrazine decomposition. *Catal today.* 2012;185(1):198–204.

[21]. Jang YB, Kim TH, Sun MH, Lee J, Cho SJ. Preparation of iridium catalyst and its catalytic activity over hydrazine hydrate decomposition for hydrogen production and storage. *Catal Today.* 2009;146(1–2):196–201.

[22]. Armstrong WE, Ryland LB, Voge HH. Catalyst comprising Ir or Ir and Ru for hydrazine decomposition. 1978;

[23]. He L, Liang B, Huang Y, Zhang T. Design strategies of highly selective nickel catalysts for H₂ production via hydrous hydrazine decomposition: a review. *Natl Sci Rev.* 2018;5(3):356–64.

[24]. Amirsardari Z, Dourani A, Amirifar MA, Massoom NG, Javadi A, Ehsani R, et al. Dentate number and functionality of O, N-donor ligands for the growth and catalytic reaction of iridium nanoparticles. *Chem Pap.* 2020;74(10):3233–41.